State space control using LQR method for a cart-inverted pendulum linearised model

Article · February 2017

CITATIONS
19

READS
14,663

5 authors, including:

Indrazno Siradjuddin
Politeknik Negeri Malang
118 PUBLICATIONS **362** CITATIONS
SEE PROFILE

Budhy Setiawan
Politeknik Negeri Malang
65 PUBLICATIONS **106** CITATIONS
SEE PROFILE

Ahmad Fahmi
State University of Malang
2 PUBLICATIONS **20** CITATIONS
SEE PROFILE

Zakiyah Amalia
Politeknik Negeri Malang
8 PUBLICATIONS **68** CITATIONS
SEE PROFILE

State space control using LQR method for a cart-inverted pendulum linearised model

Indrazno Siradjuddin[1], Budhy Setiawan[1], Ahmad Fahmi[2], Zakiya Amalia[1] and Erfan Rohadi[3]
[1]Electrical Engineering Department, Malang State Polytechnic, Malang, Indonesia
[2]Electrical Engineering Department, Malang State University, Malang, Indonesia
[3]Information Technology Department, Malang State Polytechnic, Malang, Indonesia

The Cart-Inverted Pendulum System (CIPS) is a classical benchmark control problem. Its dynamics resembles with that of many real world systems of interest like missile launchers, pendubots, human walking and segways and many more. The control of this system is challenging as it is highly unstable, highly non-linear, non-minimum phase system and underactuated. Furthermore, the physical constraints on the track position also pose complexity in its control design. This paper presents a control method to stabilise the unstable CIPS within the different physical constraints such as in track length and control voltage. A novel cart-inverted pendulum model is proposed where mechanical transmission and a dc motor mathematical model have been included which resembles the real inverted pendulum. Therefore problems emerged in realtime implementation can be minimised. A systematic the state feedback design method by choosing weighting matrices key to the Linear Quadratic Regulator (LQR) design is presented. Simulation experiments have been conducted to verify the controller's performances. From the obtained simulation and experiments it is seen that the proposed method can perform well stabilising the pendulum at the upright angle position while maintaining the cart at the desired position.

***Index Terms*—Cart-Inverted Pendulum, Linear Quadratic Regulator, Optimal Control, Non Linear System**

I. Introduction

CONTROLLING a Cart-Inverted Pendulum System (CIPS) is a challenging problem which is widely used as benchmark for testing control algorithms such as PID controllers [1], neural networks [2], [3], fuzzy control [4], genetic algorithms [5]. The CIPS features as higher order, nonlinear, strong coupling and multivariate system, which has been studied by many researchers. It is used to model the field of robotics and aerospace field, and so has important significance both in the field of the theoretical study research and practice. It has good practical applications right from missile launchers to segways, human walking, earthquake resistant building design etc. The CIPS dynamics resembles the missile or rocket launcher dynamics as its center of gravity is located behind the centre of drag causing aerodynamic instability. The CIPS has two equilibrium points [6], one of them is stable while the other is unstable. The stable equilibrium corresponds to a state in which the pendulum is pointing downwards. The control challange is to maintain the pendulum at the unstable equilibrium point where the pendulum upwards, with minimum control energy. In recent times optimal control provides the best possible solution to process control problems for a given set of performance objectives. Detail review on optimal control has been presented in [7]. Survey on optimal control approaches and their applications have been conducted, for instance, an optimal control approach for inventory systems [8] and energy optimisation [9].

This paper investigates the application of the Linear Quadratic Regulator (LQR) to stabilise the CIPS at the unstable equilibrium point. The organisation of this paper is structured as follows: The dynamic modelling using Lagrangian approach firstly discussed in Section II In this section, the state space representation of the CIPS is presented where the DC motor and its transmission system are considered. Section III discusses the LQR method in detail, followed by simulation and results of the LQR control approach applied on CIPS problem presented in Section IV Conclusion is presented in Section V

Corresponding author: Indrazno Siradjuddin (email: indrazno@polinema.ac.id).

II. System Modeling

A. Lagrange's Equation

Lagrange's equation is used to describe the motion equation of a complex system dynamic in a very efficient way. It reduces the need for complicated vector analysis that usually required for discribing forces applied on a mechanical system.

The fundamental principle of Lagrane's equation is the representation of the system by a set of generalised coordinate $\mathbf{q} = \{q_1, \cdots, q_i, \cdots, q_n\}$, where n is the total assigned generalised coordinate. q_i is an independent degree of freedom of true system which completely incorporate the contraints unique to that system, i.e., the interconnections between parts of the system.

The Lagrangian function $\mathcal{L}$ is expressed by the kinetic energy $\mathcal{K}$ and the potential energy $\mathcal{P}$ as discribed as follows

$$\mathcal{L} = \mathcal{K}(\mathbf{q}, \dot{\mathbf{q}}) - \mathcal{P}(\mathbf{q}) \tag{1}$$

where the kinetic energy function in terms of the geralised coordinate $\mathbf{q}$ and its derivative $\dot{\mathbf{q}}$. The potential energy function is expressed in terms of only the generalised coordinate.

The desired motion equations are derived using

$$\frac{\mathrm{d}}{\mathrm{d}t}\left(\frac{\partial \mathcal{L}}{\partial \dot{q}_i}\right) - \frac{\partial \mathcal{L}}{\partial q_i} = \mathcal{Q}_i \tag{2}$$

where $\mathcal{Q}_i$ denotes the external force applied in term of q_i coordinate. The expression in (2) is called Lagrange's equation. It can be deduced that for n generalised coordinates, the system dynamic is represented by n second order differential equations.

B. Lagrange's Equation of The System

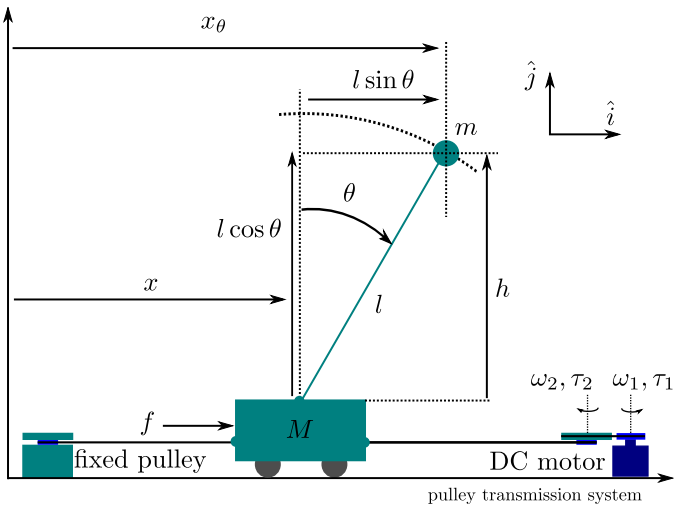

Fig. 1. The inverted pendulum on a cart system

The motion of the cart is only in $\hat{i}$ direction, thus the total kinetic energy of the cart can be expressed as

$$\mathcal{K}_M = \frac{1}{2}M\dot{x}^2 \tag{3}$$

The pendulum moves in $\hat{j}$ and $\hat{i}$ directions, therefore the total kinetic energy of the pendulum is expressed as

$$\mathcal{K}_m = \frac{1}{2}m(\dot{x}_\theta + \dot{h}) \tag{4}$$

It can be seen in Fig. 1 that

$$\begin{aligned} x_\theta &= x + l\sin\theta && (5)\\ h &= l\cos\theta && (6)\end{aligned}$$

Taking the derivative of Eq. (5) and Eq. (6), we have

$$\begin{aligned} \dot{x}_\theta &= \dot{x} + l\dot{\theta}\cos\theta && (7)\\ \dot{h} &= -l\dot{\theta}\sin\theta && (8)\end{aligned}$$

Therefore, the pendulum kinetic energy in Eq. (4) can be rewritten as

$$\begin{aligned} \mathcal{K}_m &= \frac{1}{2}m((\dot{x} + l\dot{\theta}\cos\theta)^2 + (-l\dot{\theta}\sin\theta)^2) && (9)\\ &= \frac{1}{2}m(\dot{x}^2 + 2\dot{x}l\dot{\theta}\cos\theta + l^2\dot{\theta}^2) && (10)\end{aligned}$$

hence the total kinetic energy from the cart and the pendulum can be obtained as

$$\begin{aligned} \mathcal{K} &= \mathcal{K}_M + \mathcal{K}_m && (11)\\ &= \frac{1}{2}M\dot{x}^2 + \frac{1}{2}m(\dot{x}^2 + 2\dot{x}l\dot{\theta}\cos\theta + l^2\dot{\theta}^2) && (12)\end{aligned}$$

The potentioal energy involved in the system is only from the pendulum mass m

$$\begin{aligned} \mathcal{P} &= mgh && (13)\\ &= mgl\cos\theta && (14)\end{aligned}$$

Then, the Lagrangian equation (15) can be fully defined using Eq. (12) and Eq. (14), as follows

$$\begin{aligned} \mathcal{L} &= \frac{1}{2}M\dot{x}^2 + \frac{1}{2}m(\dot{x}^2 + 2\dot{x}l\dot{\theta}\cos\theta + l^2\dot{\theta}^2)\\ &\quad -mgl\cos\theta && (15)\end{aligned}$$

The motion of the inverted pendulum on a cart can be specifically defined by the displacement of the cart in the $\hat{i}$ direction with respect to the origin and the angle of the pendulum with respect to the $\hat{j}$ direction. Hence, the system only has two degrees of freedom reprented by x and θ, the system dynamics must be expressed in terms of x and θ. Thus, x and θ can be selected as the elements of the generalised coordinate vector $\mathbf{q}$. Using this selection, the Lagrange's equation (**??**) can be expressed for each generalised coordinate:

$$\begin{aligned} \frac{\mathrm{d}}{\mathrm{d}t}\left(\frac{\partial\mathcal{L}}{\partial\dot{x}}\right) - \frac{\partial\mathcal{L}}{\partial x} &= f && (16)\\ \frac{\mathrm{d}}{\mathrm{d}t}\left(\frac{\partial\mathcal{L}}{\partial\dot{\theta}}\right) - \frac{\partial\mathcal{L}}{\partial\theta} &= 0 && (17)\end{aligned}$$

It is assumed that the external forces applied on the system is only applied on cart in $\hat{i}$ direction, there is no external torque applied on the pendulum. Deriving for each term in the differential equation in (16) and (17), it can be obtained that

$$\begin{aligned} \frac{\partial\mathcal{L}}{\partial\dot{x}} &= (M+m)\dot{x} + ml\dot{\theta}\cos\theta && (18)\\ \frac{\mathrm{d}}{\mathrm{d}t}\left(\frac{\partial\mathcal{L}}{\partial\dot{x}}\right) &= (M+m)\ddot{x} + ml\ddot{\theta}\cos\theta\\ &\quad -ml\dot{\theta}^2\sin\theta && (19)\\ \frac{\partial\mathcal{L}}{\partial x} &= 0 && (20)\end{aligned}$$

and

$$\begin{aligned} \frac{\partial\mathcal{L}}{\partial\dot{\theta}} &= ml\dot{x}\cos\theta + ml^2\dot{\theta} && (21)\\ \frac{\mathrm{d}}{\mathrm{d}t}\left(\frac{\partial\mathcal{L}}{\partial\dot{\theta}}\right) &= ml(\ddot{x}\cos\theta - \dot{\theta}\dot{x}\sin\theta)\\ &\quad +ml^2\ddot{\theta} && (22)\\ \frac{\partial\mathcal{L}}{\partial\theta} &= -m\dot{x}l\dot{\theta}\sin\theta + mgl\sin\theta && (23)\end{aligned}$$

Therefore, the Lagrange's equation for each generalised coordinate can be rewritten as

$$\begin{aligned} f &= (M+m)\ddot{x} + ml\ddot{\theta}\cos\theta - ml\dot{\theta}^2\sin\theta && (24)\\ 0 &= ml(\ddot{x}\cos\theta - \dot{\theta}\dot{x}\sin\theta) + ml^2\ddot{\theta}\\ &\quad -(-m\dot{x}l\dot{\theta}\sin\theta + mgl\sin\theta) && (25)\end{aligned}$$

It can be seen that Eq.(24) and (25) are nonlinear which have trigonometric terms $\sin()$ and $\cos()$. The controller will be designed to stabilised the pendulum vertically with small deflection of θ. Thus, it can be approximated that with small

θ, $\sin\theta \approx \theta$ and $\cos\theta \approx 1$. Deriving Eq.(24) and (25) using this approximation, one will find the quadratic terms $\dot{\theta}^2$ and $\dot{\theta}\theta$. In the small region near equilibrium, the terms $\dot{\theta}^2$ and $\dot{\theta}\theta$ are significantly small. Using aforementioned assumptions, the linearised Lagrange's equation can be obtained as follows

$$f = (M+m)\ddot{x} + ml\ddot{\theta} \quad (26)$$

$$0 = \ddot{x} + l\ddot{\theta} - g\theta \quad (27)$$

C. DC Motor: Torque, Armature Voltage and Angular Velocity Model

The armature circuit equation is

$$i_a R_a + L_a \frac{\mathrm{d}i_a}{\mathrm{d}t} + v_b = v_a \quad (28)$$

The generated back electromotive force (emf), v_b, is proportional to the rotational speed of the rotor

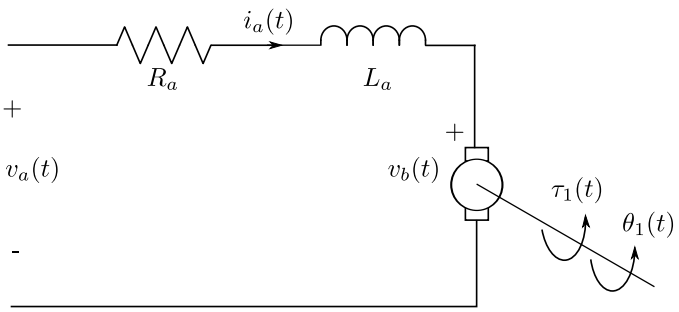

Fig. 2. DC Motor Armature Equivalent Circuit

$$v_b = K_b \frac{\mathrm{d}\theta_1}{\mathrm{d}t} \quad (29)$$

where K_b is the back emf constant and $\omega_1 = \frac{\mathrm{d}\theta_1}{\mathrm{d}t}$. The motor torque τ_1 is proportional to the armature current i_a, hence

$$\tau_1 = K_t i_a \quad (30)$$

where K_t is the motor torque constant. Substituting Eq.(29) and (30) (in term of i_a) into (28), one obtains

$$\frac{\tau_1}{K_t} R + L_a \frac{\mathrm{d}^2\tau_1}{(\mathrm{d}t)^2} + K_b \frac{\mathrm{d}\theta_1}{\mathrm{d}t} = v_a \quad (31)$$

Generally, the inductor in the rotor is small, thus can be neglected, then the armature circuit equation in term of τ_1 becomes

$$\tau_1 = -K_t \frac{K_b}{R_a}\omega_1 + \frac{K_t}{R_a} v_a \quad (32)$$

In the mechanical transmission (i.e., geared and pulley systems), it applies a following formula

$$\frac{\tau_2}{\tau_1} = \frac{N_2}{N_1} = \frac{\omega_1}{\omega_2} = \frac{r_2}{r_1} \quad (33)$$

where N is the number of a gear teeth and r is the radius of a pulley. The motor angular velocity ω_1 can be expressed in term of the cart velocity $\dot{x}$ (reffering to the Fig.1) by

$$\frac{2\pi r_2}{\dot{x}} = \frac{r_2}{r_1}\frac{2\pi}{\omega_1} \quad (34)$$

where the term $2\pi r_2$ is the circumference of the pulley that connects to the cart using a belt. Therefore,

$$\omega_1 = \frac{\dot{x}}{r_1} \quad (35)$$

Substituting Eq.(35) into Eq.(32) yields

$$\tau_1 = K_r(-K_b \frac{\dot{x}}{r_1} + v_a) \quad (36)$$

The force that moves the cart is caused by the torque τ_2, for this reason, it is needed to transform $\tau_1 \mapsto \tau_2$. Consequently, using $fr_2 = \tau_2$ (the force that perpendicular to the direction of r_2 from pulley centre), it can be verified that

$$f = \frac{K_r}{r_1}(-K_b \frac{\dot{x}}{r_1} + v_a) \quad (37)$$

where $K_r = \frac{K_t}{R_a}$. Substituting Eq.(37) into Eq.(26) produces a new Lagrange's equation in term of generalised coordinate x as follows

$$\frac{K_r}{r_1} v_a = (M+m)\ddot{x} + \frac{K_r K_b}{(r_1)^2}\dot{x} + ml\ddot{\theta} \quad (38)$$

To simplify the derivation, the following shorthands are used

$$\mathsf{c}_1 = \frac{K_r K_b}{(r_1)^2} \quad (39)$$

$$\mathsf{c}_2 = \frac{K_r}{r_1} \quad (40)$$

then from the Lagrange's equation (38), and by substituting the term $l\ddot{\theta}$ from Eq.(27) into Eq.(38), it can be obtained a following the first differential equation of the system

$$\ddot{x} = \frac{1}{M}\left(\mathsf{c}_2 v_a - \mathsf{c}_1\dot{x} - mg\theta\right) \quad (41)$$

Rearranging Eq.(27), one can derive

$$\ddot{\theta} = \frac{1}{l}\left(g\theta - \ddot{x}\right) \quad (42)$$

Substituting Eq.(41) into Eq.(42), the second differential equation of the system can be expressed as follows

$$\ddot{\theta} = \frac{1}{l}\left(g\theta - \frac{1}{M}\left(\mathsf{c}_2 v_a - \mathsf{c}_1\dot{x} - mg\theta\right)\right) \quad (43)$$

$$= -\frac{\mathsf{c}_2}{Ml} v_a + \frac{\mathsf{c}_1}{Ml}\dot{x} + \frac{(M+m)g}{Ml}\theta \quad (44)$$

At this point, the diffrential equations of the cart-pendulum motion which based on the Lagrange's method have been developed. Next step, before the optimal controller can be defined, firstly, the differential equations in the state space representation has to be formed, as discussed in the following section.

D. State Space Representation

Following equations are state space representation of a system

$$\dot{\mathbf{x}} = \mathbf{A}\mathbf{x} + \mathbf{B}\mathbf{u} \quad (45)$$

$$\mathbf{y} = \mathbf{C}\mathbf{x} + \mathbf{D}\mathbf{u} \quad (46)$$

where $\mathbf{x} \in \mathbb{R}^j$ is a state vector and j is the total number of the state variable. $\dot{\mathbf{x}}$ is the time derivative of the state vector.

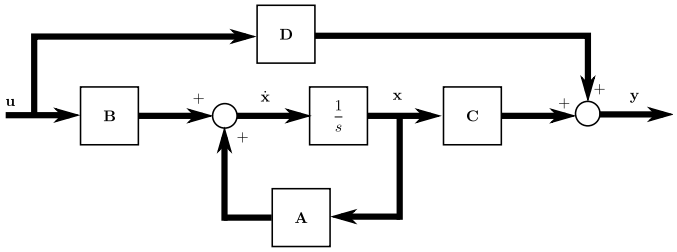

Fig. 3. Open loop system

A vector $\mathbf{u} \in \mathbb{R}^k$ is the control input or control vector which has k elements of control variables. The $\mathbf{A} \in \mathbb{R}^{j\times j}$, $\mathbf{B} \in \mathbb{R}^{j\times k}$ and $\mathbf{C} \in \mathbb{R}^{p\times j}$ are called the system, the input and the output matrices, respectively, where p is the output number. The output vector is denoted as $\mathbf{y} \in \mathbb{R}^p$. The open loop system diagram describing the state space form is shown in Fig.3.

For the case of CIPS, the state vector, its derivative and the control input are defined as $\mathbf{x} = [x\,\theta\,\dot{x}\,\dot{\theta}]^{\mathrm{T}}$, $\dot{\mathbf{x}} = [\dot{x}\,\dot{\theta}\,\ddot{x}\,\ddot{\theta}]^{\mathrm{T}}$, $u = v_a$, respectively. Composing Eq.(41) and Eq.(44) into the state space form, we have

$$\begin{aligned}
\mathbf{A} &= \begin{bmatrix} 0 & 0 & 1 & 0 \\ 0 & 0 & 0 & 1 \\ 0 & -\frac{mg}{M} & -\frac{\mathsf{c}_1}{M} & 0 \\ 0 & \frac{(M+m)g}{Ml} & \frac{\mathsf{c}_1}{Ml} & 0 \end{bmatrix}, \\
\mathbf{B} &= \begin{bmatrix} 0 \\ 0 \\ \frac{\mathsf{c}_2}{M} \\ -\frac{\mathsf{c}_2}{Ml} \end{bmatrix}, \mathbf{C} = \begin{bmatrix} 1 & 0 & 0 & 0 \\ 0 & 1 & 0 & 0 \end{bmatrix} \\
\mathbf{y} &= [x\,\theta]^{\mathrm{T}}, \mathbf{D} = \emptyset
\end{aligned}$$

It is assumed that only x and θ can be observed from sensors (e.g optical encoders) and the mapping from the state vector into the output vector is one-to-one mapping.

III. LQR METHOD

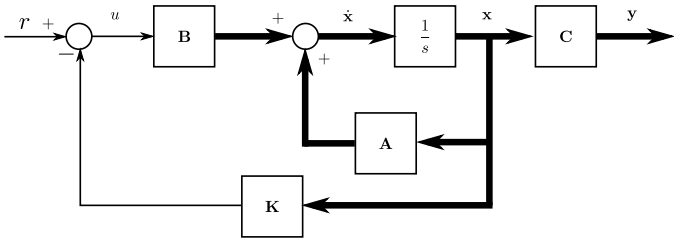

Fig. 4. Closed loop system

Linear Quadratic Regulator Controller is based on full state-feedback control principle (see Fig.4). The control gain $\mathbf{K}$ can be obtained, based on minimising the perfomance cost function described as

$$\mathcal{J} = \int_0^\infty (\mathbf{x}^T \boldsymbol{\mathcal{Q}} \mathbf{x} + u^2 \mathcal{R})\,\mathrm{d}t \tag{47}$$

where $\boldsymbol{\mathcal{Q}} \in \mathbb{R}^{j\times j}$ is a real symmetric matrix and $\mathcal{R}$ is a scalar that both should be selected. $\boldsymbol{\mathcal{Q}}$ and $\mathcal{R}$ determine the relative importance of the error and the energy cost. Therefore, the matrix $\boldsymbol{\mathcal{Q}}$ and $\mathcal{R}$ signify the trade-off between performance and control effort respectively. If $|\boldsymbol{\mathcal{Q}}|$ is relatively smaller than $\mathcal{R}$, the control system becomes expensive since $\mathcal{J}$ primarily penalises the use of control energy. In contrast, when $|\boldsymbol{\mathcal{Q}}|$ is relatively bigger than $\mathcal{R}$, the control system becomes a cheap control because an arbitrary small control effort can be used to stabilise the system, however, the system responses will be relatively slow. It is a common practice to let $\mathcal{R} > 0$ and $\boldsymbol{\mathcal{Q}}$ be a diagonal matrix in the form of

$$\boldsymbol{\mathcal{Q}} = \begin{bmatrix} q_1 & 0 & \cdots & 0 \\ 0 & q_2 & \cdots & 0 \\ \vdots & \vdots & \ddots & 0 \\ 0 & 0 & \cdots & q_j \end{bmatrix} \tag{48}$$

where $(q_1, q_2, \cdots, q_j)$ are positive values. From the Laplace transfer function of the closed loop system (Fig,4), the denominator can be found as

$$D(s) = s\mathbf{I} - (\mathbf{A} - \mathbf{BK}) \tag{49}$$

where $\mathbf{I}$ is an identity matrix. Hence, all eigenvalues of $(\mathbf{A} - \mathbf{BK})$ determine the stability and transient response characteristics of the closed loop system. The design effort is to select the feed-back gain $\mathbf{K}$ such that the eigenvalues of $(\mathbf{A}-\mathbf{BK})$ have negative real parts. The optimal feed-back gain $\mathbf{K}$ can be obtained by solving the following Riccati Equation for a positive definite matrix $\mathbf{P}$:

$$\mathbf{A}^T\mathbf{P} + \mathbf{PA} - \mathbf{PB}\mathcal{R}^{-1}\mathbf{B}^T\mathbf{P} + \boldsymbol{\mathcal{Q}} = 0 \tag{50}$$

then the optimal feed-back gain $\mathbf{K}$ can be computed as

$$\mathbf{K} = \mathcal{R}^{-1}\mathbf{B}^T\mathbf{P} \tag{51}$$

Note that if matrix $(\mathbf{A} - \mathbf{BK})$ is a stable matrix then $\mathbf{P}$ always exists. In contrast, for the case of an unstable matrix $(\mathbf{A} - \mathbf{BK})$, the matrix $\mathbf{P}$ does not exist for solving Eq.(50). Thus, it is necessary for the control engineer to check the controllability and observability of the system model beforehand the controller implementation. The controllability means that for any initial state values, the acceptable control effort u can steer the state to any final state values within some finite time window if only if rank($\boldsymbol{\mathcal{C}}$) is equal to the number of state variables.

$$\boldsymbol{\mathcal{C}} = \left[\mathbf{A}|\mathbf{AB}|\mathbf{A}^2\mathbf{B}|\cdots|\mathbf{A}^{j-1}\mathbf{B}\right] \tag{52}$$

$$\mathrm{rank}(\boldsymbol{\mathcal{C}}) = j \tag{53}$$

Observability is a property of the plant with appropriate sensor selection without considering actuator selection. To test that the system is an observable system, the rank of observability matrix $\boldsymbol{\mathcal{O}}$ has to be equal to the number of the state. The observability matrix $\boldsymbol{\mathcal{O}}$ can be computed as

$$\boldsymbol{\mathcal{O}} = \left[\mathbf{C}|\mathbf{CA}|\mathbf{CA}^2|\cdots|\mathbf{CA}^{j-1}\right] \tag{54}$$

The aforementioned detail for obtaining the feed-back gain $\mathbf{K}$ does not guarantee that the obtained $\mathbf{K}$ can give the steady state error $\mathbf{e} = \mathbf{0}$. For a unit step reference input, it is very often that the transfer function $T(s)$ of a closed loop has

unsastifactory dc gain N, $0 < N < 1$. The transfer function of a closed loop system shown in Fig.4 is expressed as

$$T(s) = \mathbf{C}(s\mathbf{I} - (\mathbf{A} - \mathbf{BK}))^{-1}\mathbf{B} \tag{55}$$

where dc gain N can be obtained by $T(s)|_{s=0}$. The solution to improve the performance of the steady state error is to put a pregain $\bar{N}$ in the system as depicted in Fig.5. The pregain $\bar{N}$ is computed as $\bar{N} = \frac{1}{N}$. The full state space equation can be expressed as

$$\begin{aligned} \dot{\mathbf{x}} &= (\mathbf{A} - \mathbf{BK})\mathbf{x} + \mathbf{B}u & (56)\\ \mathbf{y} &= \mathbf{Cx} & (57)\\ u &= r - \mathbf{Kx} & (58) \end{aligned}$$

where $\mathbf{K} \in \mathbb{R}^j$.

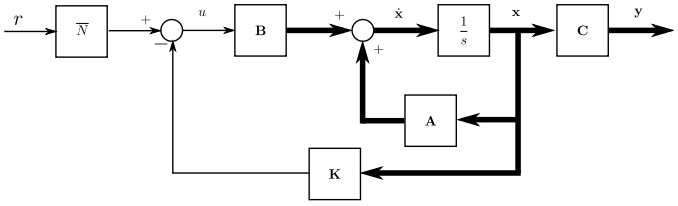

Fig. 5. Closed loop system with pregain

IV. Simulation and Results

In order to simulate the full state feed-back control system, the defined system parameters in Table I are used. The resulting eigenvalues of the open loop system depicted in Fig.3 are $\{0, 6.5681, -6.5718, -0.0364\}$ which can be obtained by $\det(s\mathbf{I} - \mathbf{A})$. It can be seen that the open loop system has a positive real part, therefore, the system is an unstable system. However, using the system state space described in Eq.(45) and (46), the CIPS is a completely controllable and observable since the matrix ranks of $\boldsymbol{\mathcal{C}}$ and $\boldsymbol{\mathcal{O}}$ are both equal to the number of the state, rank($\boldsymbol{\mathcal{C}}$) = rank($\boldsymbol{\mathcal{O}}$) = 4, which can be verified using results shown in Eq.(59) and Eq.(60).

TABLE I
THE CIPS PARAMETERS

No.	Parameter	Value	Units
(1)	R_a	1	Ω
(2)	K_t	0.02	N · m/A
(3)	K_b	0.02	V · s/rad
(4)	r_1	0.015	m
(5)	M	1	Kg
(6)	m	0.1	Kg
(7)	l	0.25	m

$$\boldsymbol{\mathcal{C}} = \begin{bmatrix} 0 & 0.200 & -0.008 & 0.785 \\ 0 & -0.800 & 0.032 & -34.533 \\ 0.200 & -0.008 & 0.785 & -0.063 \\ -0.800 & 0.032 & -34.533 & 1.507 \end{bmatrix} \tag{59}$$

$$\boldsymbol{\mathcal{O}} = \begin{bmatrix} 1 & 0 & 0 & 0 \\ 0 & 1 & 0 & 0 \\ 0 & 0 & 1 & 0 \\ 0 & 0 & 0 & 1 \\ 0 & -0.981 & -0.040 & 0 \\ 0 & 43.164 & 0.160 & 0 \\ 0 & 0.039 & 0.002 & -0.981 \\ 0 & -0.157 & -0.006 & 43.164 \end{bmatrix} \tag{60}$$

The first design choice of $\boldsymbol{\mathcal{Q}}$ and $\mathcal{R}$ in the performance cost function are $\boldsymbol{\mathcal{Q}} = \mathbf{C}^T\mathbf{C} = \text{diag}\{1, 1, 0, 0\}$ and $\mathcal{R} = 1$. It can be noted that the elements of matrix $\boldsymbol{\mathcal{Q}}$; $\{q_1, q_2\} = \{1, 1\}$ means that the design choice control effort tries to make an equal emphasis between state x and θ regardles the condition of state $\dot{x}$ and $\dot{\theta}$. Furthermore, the initial choice of $\boldsymbol{\mathcal{Q}}$ ensures that $\mathbf{x}^T\boldsymbol{\mathcal{Q}}\mathbf{x}$ is a positive semi definite matrix, for all $\mathbf{x}$. The feedback gain $\mathbf{K}$, the characteristic polynomial function $D(s)$ and its roots are found as follow

$$\begin{aligned} \mathbf{K} &= \{-1, -118.32, -3.83, -18.09\} \\ D(s) &= s^4 + 13.75s^3 + 51.29s^2 \\ &\quad +28.47s + 7.85 \\ \mathbf{s} &= \{-6.57 + 0.06\text{i}, -6.57 - 0.06\text{i}, \\ &\quad -0.3 + 0.3\text{i}, -0.3 - 0.3\text{i}\} \end{aligned} \tag{61}$$

TABLE II
LQR PARAMETERS FOR FIG.6

No.	q_1	q_2	$\mathcal{R}$
(1)	1	1	1
(2)	2	0.1	1
(3)	0.1	2	1
(4)	2	2	10

Based on the performance results of the first choice, then $\boldsymbol{\mathcal{Q}} = \{q_1, q_2, 0, 0\}$ and $\mathcal{R}$ were varied to see the effect of the variations. Table II shows the variation of $\boldsymbol{\mathcal{Q}}$ and $\mathcal{R}$. Note that in this simulation the pregain was not used. The corresponding output trajectories (x and θ) are depicted in Fig.6. The trajectory of the cart position for configuration number (1) in Table II is shown as $\bar{x}_1$ plot line in Fig.6 and likewise for the the rest of the other three configurations.

It is shown that on both Fig.6(a) and Fig.6(b) the controller can stabilise the state, cart position and pendulum angle, respectively. The controller can regulate the pendulum angle, however, the final cart position is not at the desired position ($r = 0.25$ m). The configuration of $q_1 = 2$, $q_2 = 0.1$ and $\mathcal{R} = 1$ (configuration (2)) gives the best performance since it has the smallest steady state tracking error of the cart position and the fastest regulation response of the pendulum angle. By letting q_1 relatively greater than q_2, it means that the control effort prioritses the improvement steady state of the pendulum angle. Using configuration (2), The feedback gain $\mathbf{K}$, the characteristic polynomial function $D(s)$ and its roots

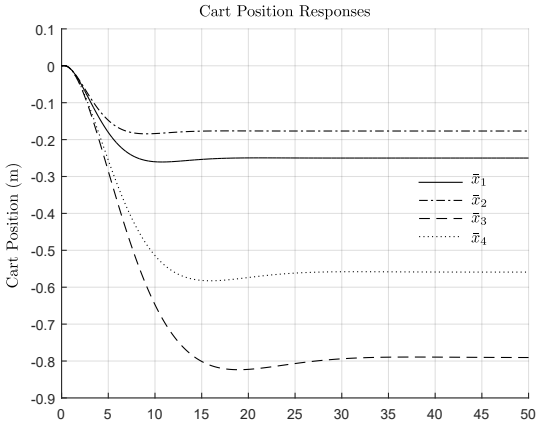

(a) Cart position response trajectories

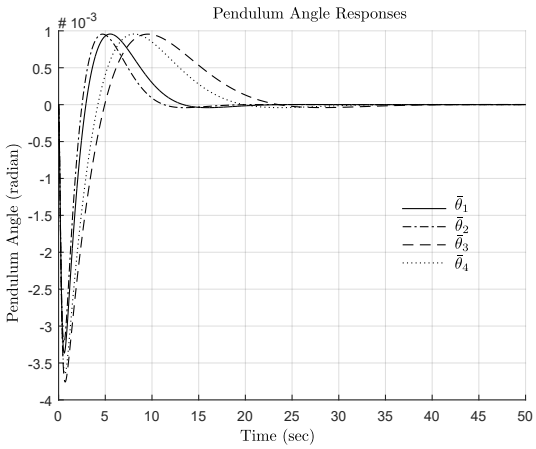

(b) Pendulum angle response trajectories

Fig. 6. State responses without pre-gain

are found as follow

$$\begin{aligned} \mathbf{K} &= \{-1.41, -120.38, -4.58, -18.42\} \\ D(s) &= s^4 + 13.86s^3 + 52.86s^2 \\ &\quad +34.38s + 11.1 \\ \mathbf{s} &= \{-6.57 + 0.02\text{i}, -6.57 - 0.02\text{i}, \\ &\quad -0.36 + 0.36\text{i}, -0.36 - 0.36\text{i}\} \end{aligned} \tag{62}$$

The configuration (2) in Table II was chosen as a starting point eliminating the steady state error for the next simulation experiment where the pregain was used implementing a closed system in Fig.5. In this simulation scheme, $\mathcal{R}$ was varied and $\boldsymbol{\mathcal{Q}}$ was kept the same, as shown in Table III. The simulation result is depicted in Fig.7.

By adding the pregain, the steady state tracking error of the cart position is eliminated for all configuration in Table III in which the desired position of the cart is reached ($r = 0.25\,\text{m}$) (see Fig.7(a)). The transient time of the cart position response is improved slightly by reducing $\mathcal{R}$. However, reducing $\mathcal{R}$ also increases the overshoot of the pendulum angle response as shown in Fig.7(b). Furthermore, reducing $\mathcal{R}$ makes $|\boldsymbol{\mathcal{Q}}|$ relatively bigger than $\mathcal{R}$, the control system penalises the use of the control effort u. Referring to Table III and Fig.7(c), the

TABLE III
LQR PARAMETERS FOR FIG.7

No.	q_1	q_2	$\mathcal{R}$
(1)	2	0.1	0.01
(2)	2	0.1	0.001
(3)	2	0.1	0.0001
(4)	2	0.1	0.00001

required control input voltage is higher when $\mathcal{R}$ is smaller. For instance, the smallest $\mathcal{R} = 0.00001$ requires the control input of 115 volts. In this configuration, the feedback gain $\mathbf{K}$, the pregain, the characteristic polynomial function $D(s)$ and its roots are found as follow

$$\begin{aligned} \mathbf{K} &= \{-447.2, -333.5, -174.9 - 50.7\} \\ \bar{N} &= -447.21 \\ D(s) &= s^4 + 60s^3 + 1730s^2 \\ &\quad +13574s + 35097 \\ \mathbf{s} &= \{-24.8 + 24.2\text{i}, -24.8 - 24.2\text{i}, \\ &\quad -5.1 + 1.9\text{i}, -5.1 - 1.9\text{i}\} \end{aligned} \tag{63}$$

Further simulation experiments were conducted to fine tune the LQR parameters to obtain the fastest transient response where the controller input was contrained with the maximum value of 15 volts (half of the maximum voltage of the DC motor). The configurations used in these simulations are listed in Table IV. It can be seen on the Fig.8 that configuration (3)

TABLE IV
LQR PARAMETERS FOR FIG.8

No.	q_1	q_2	$\mathcal{R}$
(1)	2	0.1	0.01
(2)	2	0.01	0.01
(3)	4	0.1	0.01
(4)	4	0.5	0.00001

is the most satisfactory result which met the desired criteria. In this final configuration, the feedback gain $\mathbf{K}$, the pregain, the characteristic polynomial function $D(s)$ and its roots are found as follow

$$\begin{aligned} \mathbf{K} &= \{-63.25, -69.54 - 30.83 - 10.91\} \\ \bar{N} &= -63.2456 \\ D(s) &= s^4 + 31.2s^3 + 434.2s^2 \\ &\quad +2364.4s + 4963.5 \\ \mathbf{s} &= \{-11.4 + 9.5\text{i}, -11.4 - 9.5\text{i}, \\ &\quad -4.2 + 2.2\text{i}, -4.2 - 2.2\text{i}\} \end{aligned} \tag{64}$$

V. CONCLUSIONS

The dynamic modeling and control system design of a complex dynamic system such as the CIPS has been successfully conducted. The CIPS dynamic model was analysed using Lagrangian approach. The control system design process

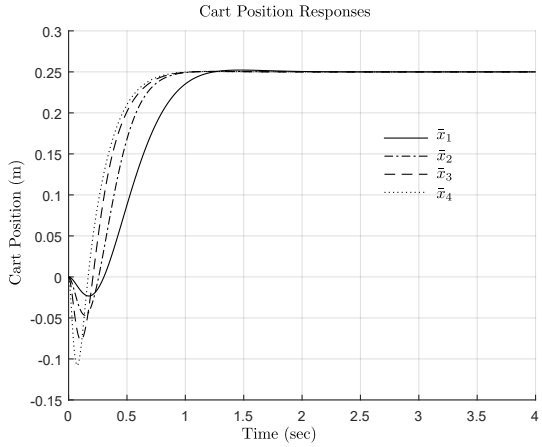

(a) Cart position response trajectories

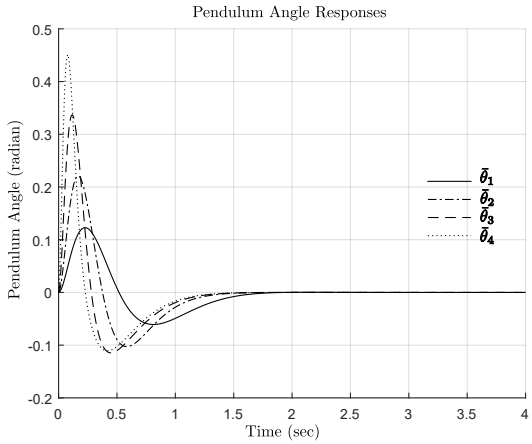

(b) Pendulum angle response trajectories

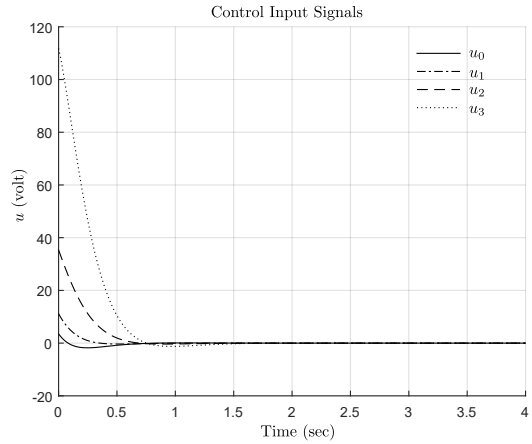

(c) Control ouput trajectories

Fig. 7. State responses with pre-gain

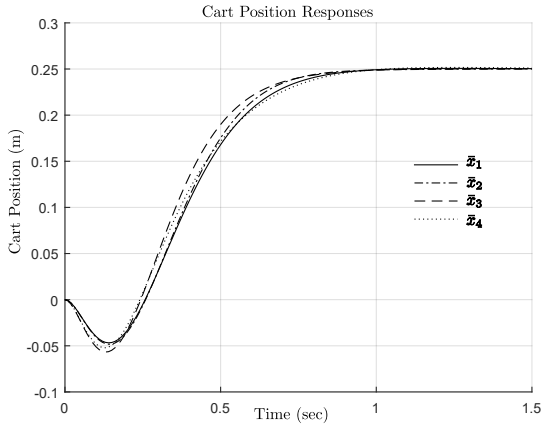

(a) Cart position response trajectories

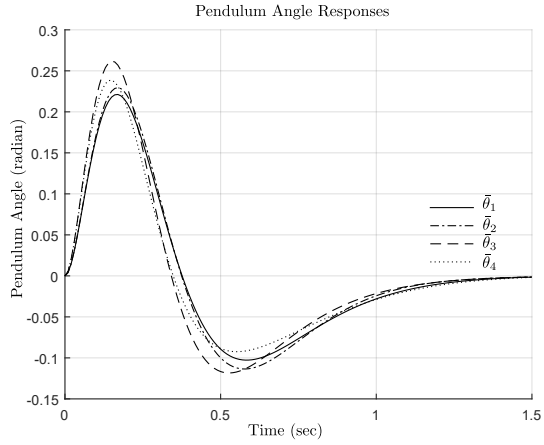

(b) Pendulum angle response trajectories

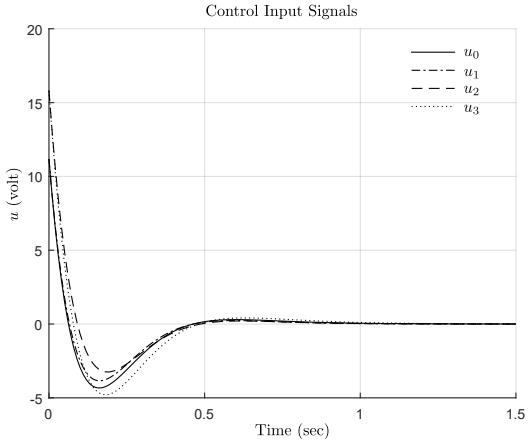

(c) Control ouput trajectories

Fig. 8. State responses with pre-gain

involved state-feedback simulation after determining the controllability and observability of the system. It was assumed that the cart position x and the pendulum angle θ where available from sensor measurements. Hence, it was determined that by giving two sensor measurements was sufficient to construct a state-feedback system observable. Determining the gain matrix $\mathbf{K}$ was the important step in the optimal control design. The optimality of the resulted gain matrix $\mathbf{K}$ was analysed by the performance cost function $\mathcal{J}$. The parameters in the performance cost function, the LQR weights $\boldsymbol{\mathcal{Q}}$ and $\mathcal{R}$ were manually selected, knowing that the trade-off between the performance and the control effort were determined by the selection of $\boldsymbol{\mathcal{Q}}$ and $\mathcal{R}$. Regardless, the values of $\boldsymbol{\mathcal{Q}}$ and $\mathcal{R}$, the cost function has a unique minimum that can be obtained

by solving the Riccati Equation.
It is important to be noted that for the case of the tracking performance, where the controller effort should make $y(t) \approx r(t)$ as $t \to \infty$, hence the DC gain of the transfer function should be approximately 1. Therefore, it is necessary to scale the reference input using pregain $\bar{N}$. Simulation experiments were systematically conducted by varying the configuration of $\mathcal{Q}$ and $\mathcal{R}$. Simulation results have been discussed in detail. The simulation results have shown that the larger $\mathcal{Q}$ and $\mathcal{R}$ the more you penalize the state and the control effort. Choosing a large value for $\mathcal{R}$ means that the controller stabilises the system with less (weighted) energy, it is called expensive control strategy. This control strategy is used when the control signal is constrained . On the contrary, choosing a small value for $\mathcal{R}$ means that the controller penalises the control signal (cheap control strategy), causing a large control signal. Large $\mathcal{Q}$ implies less concern about the changes in the states.

ACKNOWLEDGMENT

Published results were acquired with the support of Ministry of Research and Technology and Higher Education of Indonesia.

REFERENCES

[1] C. Wang, G. Yin, C. Liu, and W. Fu, "Design and simulation of inverted pendulum system based on the fractional pid controller," in *2016 IEEE 11th Conference on Industrial Electronics and Applications (ICIEA)*, June 2016, pp. 1760–1764.

[2] Z. Pengpeng, Z. Lei, and H. Yanhai, "Bp neural network control of single inverted pendulum," in *Proceedings of 2013 3rd International Conference on Computer Science and Network Technology*, Oct 2013, pp. 1259–1262.

[3] M. H. Arbo, P. A. Raijmakers, and V. M. Mladenov, "Applications of neural networks for control of a double inverted pendulum," in *12th Symposium on Neural Network Applications in Electrical Engineering (NEUREL)*, Nov 2014, pp. 89–92.

[4] G. O. Tirian, O. Prostean, I. Filip, and C. Rat, "Inverted pendulum controlled through fuzzy logic," in *2015 IEEE 10th Jubilee International Symposium on Applied Computational Intelligence and Informatics*, May 2015, pp. 85–90.

[5] N. Metni, "Neuro-control of an inverted pendulum using genetic algorithm," in *2009 International Conference on Advances in Computational Tools for Engineering Applications*, July 2009, pp. 27–33.

[6] R. F. Harrison, "Asymptotically optimal stabilising quadratic control of an inverted pendulum," *IEE Proceedings - Control Theory and Applications*, vol. 150, no. 1, pp. 7–16, Jan 2003.

[7] D. Tabak, "Applications of mathematical programming techniques in optimal control: A survey," *IEEE Transactions on Automatic Control*, vol. 15, no. 6, pp. 688–690, Dec 1970.

[8] P. Ignaciuk and A. Bartoszewicz, "Linear-quadratic optimal control of periodic-review perishable inventory systems," *IEEE Transactions on Control Systems Technology*, vol. 20, no. 5, pp. 1400–1407, Sept 2012.

[9] A. I. Bratcu, I. Munteanu, and E. Ceanga, "Optimal control of wind energy conversion systems: From energy optimization to multi-purpose criteria - a short survey," in *2008 16th Mediterranean Conference on Control and Automation*, June 2008, pp. 759–766.